Mechanism of active eruption of molars in adolescent rats

Takashi Oikawa*, Yoshiaki Nomura**, Chihiro Arai*, Koji Noda*, Nobuhiro Hanada** and Yoshiki Nakamura*

Departments of *Orthodontics and **Translational Research, School of Dental Medicine, Tsurumi University, Yokohama, Japan

Correspondence to: Takashi Oikawa, School of Dental Medicine, Tsurumi University, 2-1-3 Tsurumi, Tsurumi-ku, Yokohama 230-8501, Japan. E-mail: oikawa-t@tsurumi-u.ac.jp

SUMMARY The mechanism of active eruption of molars was examined in 36 male adolescent Wistar rats. Histological, histochemical [tetracycline (TC) labelling and alkaline phosphatase (ALP) activity], and immunohistochemical [transforming growth factor (TGF)-β1, -β2, and -β3] investigations were conducted of the rat molar areas. Real-time reverse transcription–polymerase chain reaction (RT-PCR) for mRNA of TGF-β was performed on the periodontal ligament (PDL) dissected out by laser capture microdissection.

TC labelling lines showed that a considerable amount of bone formation occurred in the alveolar crest region, apical region, and intraradicular septum, indicating that the maxillary molars had moved downward. However, the periodontal fibres revealed a regular arrangement (alveolar crest, horizontal and oblique fibres) during the experimental period. This suggests that new formation of alveolar crest fibres and rearrangement of the periodontal fibres occurred in the PDL. ALP activity was intense on the bone surface and in the PDL. TGF-β1 was also detected in osteoblasts and fibroblasts but less so in cementoblasts. Real-time RT-PCR also demonstrated significant expression of mRNA of TGF-β1 in the PDL, indicating that TGF-β1 was involved in active eruption. These results suggest that active eruption occurs in adolescent rats and can be managed by TGF-β1.

Introduction

Vertical growth of the jaws and increase in face height continue even after transverse and antero-posterior growth is complete (Graber, 1972). Vertical growth induces active eruption (Proffit and Fields, 2000) of posterior teeth, which continues after completion of eruption and root formation. In fact, superimposition of cephalometric tracings, at the palatal and mandibular planes, demonstrated that maxillary first molars move downward and mandibular first molars move upward even in adolescence. The movement of molars has been noted as vertical growth of molars or growth of the posterior alveolar process of the jaws, causing the molar teeth to move away from the palatal or mandibular plane (Schudy, 1965). This has also been noted as vertical drift of molars in their own sockets or passive carrying of the dental arch as a whole, and both vertical drift and passive carrying proceed simultaneously (Enlow, 1990). These phenomena also continue in late adolescence in humans, which is an optimal period for orthodontic treatment. However, there have been few studies on active eruption occurring during that period by vertical growth of the jaws because this had been confused with 'passive eruption' defined as actual migration of the attachment without any eruption of the tooth. It is important to gather information on active eruption in this period in order to understand bite raising or bite deepening by way of elongation and depression of the teeth in the orthodontic treatment of growing adolescent patients.

In the mechanism of the active eruption, periodontal tissues inevitably play important roles. In particular, the rearrangement of the periodontal fibres and formation of alveolar bone are mainly involved in the mechanism. This mechanism may also be regulated by several cytokines such as transforming growth factor (TGF)-β; therefore, this study was performed to elucidate the mechanism of active eruption in relation to the alveolar bone and periodontal ligament (PDL).

Materials and methods

This study was approved by the Committee on Ethics of Tsurumi University.

Thirty-three male (10-week-old) and three male (13-week-old) Wistar strain rats were used in this study. The animals were kept in groups of three to four per cage and fed with a diet of pellets and water. The rats were divided into two groups: freeze-fixed group (30 rats) for tetracycline (TC) labelling, histochemistry, immunohistochemistry, and real-time reverse transcription–polymerase chain reaction (RT-PCR) and formalin-fixed group (6 rats) for haematoxylin–eosin (HE), Azan, and Masson staining.

Freeze-fixed group

In five rats in the freeze-fixed group, a single injection of TC (1.5 mg/100 g body weight) was administered intraperitoneally.

Three weeks later, the animals were killed, under Nembutal anaesthesia, and the maxilla of all 30 rats were dissected out and rapidly immersed in liquid nitrogen. The enamel above the gingival sulcus was removed and the frozen tissues were trimmed with a dental diamond disk in the frozen condition into smaller blocks containing the first molar. The frozen tissues were then embedded in pre-cooled optimum cutting temperature (OCT) compound (Miles Inc., Torrance, California, USA) and returned to liquid nitrogen until the OCT compound was completely frozen. The frozen blocks were stored in a refrigerator at −80°C until use. They were then mounted on stubs pre-cooled at −25°C in a cryostat (Reitz, Nussloch, Germany) with OCT compound and frontally sectioned (Nakamura *et al.*, 1994) using a super-hard tungsten steel knife (Meiwa Shoji Ltd., Tokyo, Japan). Serial frontal sections, 5 μm thick, were collected individually with powerful adhesive tape according to the method of Kawamoto (2003) and then freeze-dried for 1 hour in a cryostat.

Histology and TC labelling   The tape with the attached section from the five TC-injected rats was transferred to glass slides. For orientation, some sections were fixed with buffered formalin for 60 seconds, washed carefully with distilled water (DW), stained with 0.5 per cent toluidine blue for 1 minute at room temperature, and mounted under a coverslip with glycerin.

The sections were observed under a light and a fluorescent microscope (Olympus AX 80; Olympus Co. Ltd., Tokyo, Japan) using ultraviolet illumination to detect the uptake of TC.

Histochemistry of alkaline phosphatase activity   The sections from the freeze-fixed group were pre-fixed with 100 per cent ethanol for 60 seconds and rinsed with DW. They were then incubated in the medium of alkaline phosphatase (ALP) activity (azo dye method; Mayahara *et al.*, 1969) for 90 seconds at room temperature. After incubation, both sections were post-fixed with buffered formalin.

Immunohistochemistry of TGF-β1, 2, and 3   TGF-β1, 2, and 3 were detected by means of polyclonal rabbit primary antibodies (Santa Cruz Biotechnology, Santa Cruz, California, USA). Each of the primary antibodies was diluted 1:60 with 1.5 per cent goat serum in a phosphate-buffed solution.

Some sections were fixed with 100 per cent ethanol for 5 minutes and incubated in H_2O_2 to quench endogenous peroxidase activity for 5 minutes and then blocked with normal rabbit serum for 60 minutes at room temperature. They were incubated with rabbit primary antibodies of TGF-β1, 2, and 3 (Santa Cruz Biotechnology), respectively, for 30 minutes. Biotinylated secondary incubations were then performed followed by avidin–biotinylated horseradish

peroxidase according to the rabbit ABC Staining Systems (Santa Cruz Biotechnology).

Real-time reverse transcription–polymerase chain reaction   RT-PCR for TGF-β1, 2, and 3 was performed. Serial frontal sections, 7 μm thick, were used for this experiment. The sections were fixed with methanol for 3 minutes, stained with toluidine blue for 10 seconds, and washed with DW (ultra pure DW DNAse, RNAse free; Invitrogen Corporation, San Diego, California, USA). They were then transferred to the specimen stage of a microscope with a laser capture microdissection system (Palm Microlaser Technologies AG, Bernried, Germany). Outlines of the laser radiation were determined a few cell layers away from the calcified bone and cementum; the osteoblasts and cementoblasts were thus not included. The PDL was laser captured and microdissected from the sections and collected and immersed in denaturing solution (Nakamura *et al.*, 2007). Then, 20 μl of 2 M sodium acetate, 220 μl of phenol, and 60 μl of chloroform and isoamyl alcohol were added and stirred and centrifuged at 12 000 rpm at 4°C. Subsequently, RNA was precipitated by isopropanol and washed by 75 per cent ice-cold ethanol.

The samples were kept in 200 μl denaturing buffer (guanidium thiocyanate 0.45 mg/l, 0.5 g/l Sarcosyl, 0.025 M sodium citrate, and B-mercaptoethanol 8 μl/ml) and placed on ice. Then, 20 μl of 2 M sodium acetate, 220 μl of water-saturated phenol (Sigma, St Louis, Missouri, USA), and 60 μl of chloroform/isoamyl alcohol 24:1 (Sigma) were added. After keeping the samples on ice for 15 minutes, they were centrifuged at 1500 rpm for 15 minutes at 4°C. Then, 100 μl of the supernatant was transferred to another tube, 1 μl of glycogen (10 mg/ml; Funakoshi Co., Ltd, Tokyo, Japan) and 200 μl of isopropanol were added, and the mixture was kept at −80°C for 16 hours. The samples were centrifuged at 1500 rpm for 30 minutes at 4°C. The RNA pellets were washed with 70 per cent ethanol.

Four different oligonucleotide primer sets [TGF-β1, 2, 3 and glyceraldehyde 3-phosphate dehydrogenase (GAPDH)], used for one-step RT-PCR, were derived from a published sequence (Zhao *et al.*, 1995; Shaddy *et al.*, 1996). The sequences (5′–3′) of forward and reverse primers were CTAATGGTGGACCGCAACAAC and CGGTTCATGTC ATGGATGGTG for TGF-β1, AAAATGCCATCCCGCCC ACTT and CATCAATACCTG CAAATCTCG for TGF-β2, TGGCGGAGCACAATGAACTGG and CCTTTGAATTT GATTTCCATC for TGF-β3, and GATGCTGGTGCTGAG T ATGTCG and GTGGTGCAGGATGCATTGCTGA for GAPDH.

Real-time one-step RT-PCR assay for each gene target was performed on the total RNA samples and serial dilutions of known amounts of total RNA standards were prepared for generating a standard curve in 96-well optical plates on an ABI Prism 7900HT Sequence Detection system (Applied Biosystems, Foster, California, USA). Fifty microlitres of reaction mixture contained 25 μl of QuantiTect SYBR

Green RT-PCR Master Mix (Qiagen Inc., Valencia, California, USA), 0.5 µl specific target gene primers (0.5 µM), 0.5 µl QuantiTect RT Mix, and 1 µl of either RNA samples or target RNA standards. PCR parameters were 50°C for 30 minutes, 95°C for 15 minutes, 45 cycles of 94°C for 15 seconds, 58°C for 30 seconds, and 72°C for 30 seconds.

For each sample, an amplification plot was generated, displaying an increase in the reporter dye fluorescence (ΔRn) with each cycle of PCR. From each amplification plot, a threshold cycle (C_t) value was calculated, which was the PCR cycle number at which fluorescence was detected above the threshold, based on the variability of baseline data in the first 15 cycles. Each C_t value was used to calculate the initial amount of target mRNA based on the line equation derived from the respective standard curve. The standard curve for each gene was plotted showing C_t versus the logarithmic value of diluted concentrations of total RNA standard. If the fluorescence signal was not detected within 45 cycles, the sample was considered negative.

To correct for possible differences in the efficiency of the RT reactions, PCR amplification was performed for the housekeeping gene GAPDH and the standard curve was obtained. Likewise, the amount of endogenous GAPDH mRNA was quantified and found to be identical among all samples studied. Thus, it was considered that the GAPDH mRNA was an appropriate internal control as in a previous study (Arai *et al.*, 2005) and normalized the amount of target mRNA relative to the amount of GAPDH mRNA. Here, the amount of target mRNA was represented by the normalized value (i.e. target mRNA/GAPDH mRNA).

Formalin-fixed group

Three 10-week-old and three 13-week-old rats in the formalin-fixed group were perfused through the ascending aorta with phosphate-buffered 10 per cent formalin solution (pH 7.2, 4°C) for 15 minutes and the maxillae were resected and immersed in the same fixative at 4°C overnight. After fixation, they were trimmed into small blocks containing the first molar and decalcified with 5.0 per cent ethylenediaminetetraacetic acid-Na^2 (pH 7.2, 4°C) solution containing 7.0 per cent sucrose for 3 weeks. The blocks were then washed with DW, dehydrated with graded ethanol series, and embedded in paraffin. The blocks were cut frontally and 5 µm sections were stained with HE. The adjacent sections were also stained with Azan and Masson.

Results

Undecalcified frozen sections cut at the disto-buccal and disto-lingual roots almost perpendicular to the occlusal plane showed good structural preservation of periodontal

tissues. The structural relationships among the roots, PDL, and alveolar bone were well retained. The PDL was interposed between the roots and the alveolar bone. The width of the ligament was approximately even (Figure 1a). On the periosteal side, many osteoblasts were present on a layer of osteoid, which showed metachromasia on the calcified bone (Figure 2b).

TC labelling lines were observed in the same section under fluorescence microscopy. They were located some distance away from the bone surface and the new bone formed over the course of 3 weeks following injection could be distinguished (Figure 1b). The thickness of the bone produced over the 3 week period showed site-specific variation. Thicker bone was characteristically observed at the buccal and lingual alveolar crest regions (Figure 1c and 1d), root apex regions (Figure 1e and 1f), and intraradicular septum (Figure 1g), where TC lines were distinct. TC lines were also observed in the alveolar bone on the periosteal side, but not in the cementum, except for a trace in apical cementum.

ALP activity was localized in the whole PDL, the periosteum of the alveolar bone on both sides, the connective tissues of the alveolar crest area, and the pulp (Figure 2a). Site-specific variations in the intensity of enzyme activity were observed (Figure 2c); the activity was very high along the bone surface where the osteoblasts were located (Figure 2b) but not as high in the middle third of the PDL. On the periosteal side, a band of intense activity was detected along the bone surface, which corresponded to the osteoblastic layer. In contrast to the PDL, no ALP activity was observed in the subperiosteal connective tissues.

Immunohistochemistry of TGF-β1, 2, and 3 demonstrated different distributions. TGF-β was observed in contrast to the morphological findings (Figure 3a–e). TGF-β1 was located in the osteoblasts on the bone surface and in most fibroblasts scattered in the PDL (Figure 3c). It was also detected in the cementoblasts on the cementum surface but its immunoreactivity was weak. Neither TGF-β2 nor 3 was detected on the bone surface, in the PDL, or on the cementum surface (Figure 3d and 3e). They were not detected in the osteoblasts, fibroblasts, or cementoblasts.

Real-time RT-PCR clearly demonstrated that the PDL fibroblasts had a large volume of expression of mRNA of TGF-β1. The amount of mRNA of TGF-β1 was 5.5 times that of GAPDH. However, mRNA of TGF-β2 and 3 were not detected in the fibroblasts of the PDL (Table 1).

In the decalcified sections, the structural relationships of the periodontal tissues were same as the undecalcified sections, except that the enamel had disappeared during decalcification (Figure 4a and 4b). Every section from the 10- and 13-week-old rats showed the same findings in the periodontal fibres. The PDL had a well-developed periodontal fibre network architecture, which connected the tooth and alveolar bone. Each of the periodontal fibres was well-defined and had a wavy configuration in a
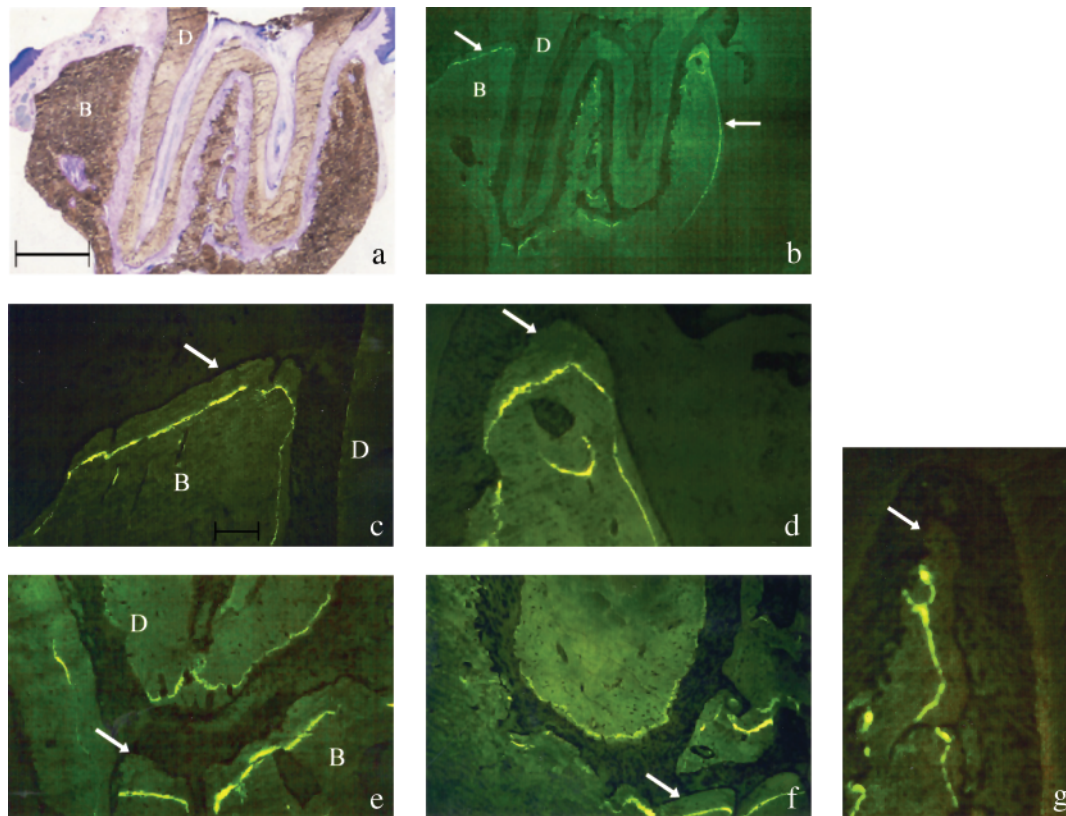
Figure 1   Periodontal tissues of the maxillary first molar. (a) Overall view of a maxillary first molar and the alveolar bone in an undecalcified section, which was cut at the disto-buccal and disto-lingual roots almost perpendicular to the occlusal plane. The structural relationships among roots, periodontal ligament, and alveolar bone were well retained. (b) Tetracycline (TC) labelling lines (arrows) demarcated new from old alveolar bone. TC lines (arrows) were more distinct at the lingual (c) and buccal (d) alveolar crest areas, root apex areas (e and f), and intraradicular septum (g), indicating that a considerable amount of bone had formed. The large arrow indicates the downward direction. (a) toluidine blue staining, ×20 (bar: 500 μm). (b) ×20. (c, d, e, f, and g) ×100 (bar: 20 μm). B, bone; D, dentine.
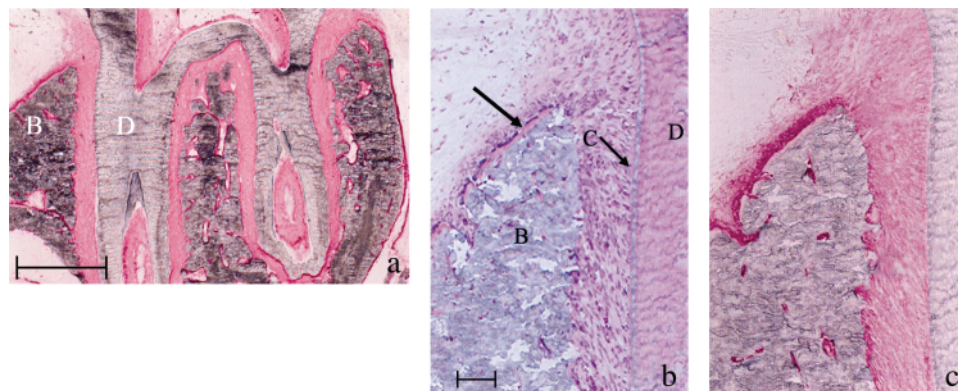

Figure 2   Alkaline phosphatase (ALP) activity in the periodontal tissues. (a) ALP activity was present in the whole periodontal ligament (PDL), periosteum of the alveolar bone on both sides, the connective tissues of the alveolar crest area, and pulp. (b) The alveolar crest area showed metachromatically stained osteoid (arrow) along the calcified bone on the periosteal side. (c) ALP activity was very high along the bone surface but not so high in the middle third of the PDL and cementum surface. A band of intense activity was present along the bone surface on the periosteal side. The large arrow indicates the downward direction. (a) ×20 (bar: 500 μm). (b and c) ×100 (bar: 20 μm). B, bone; D, dentine.

functional arrangement. Fibroblasts were spindle shaped and were arranged along the periodontal fibres. Osteoblasts were observed on the bone surface among the Sharpey's fibres.

The fibres in the cervical region were firmly embedded in the cementum and bone and extended regularly with interlacing among them from the cementum to the more apically positioned alveolar crest. However, in the middle
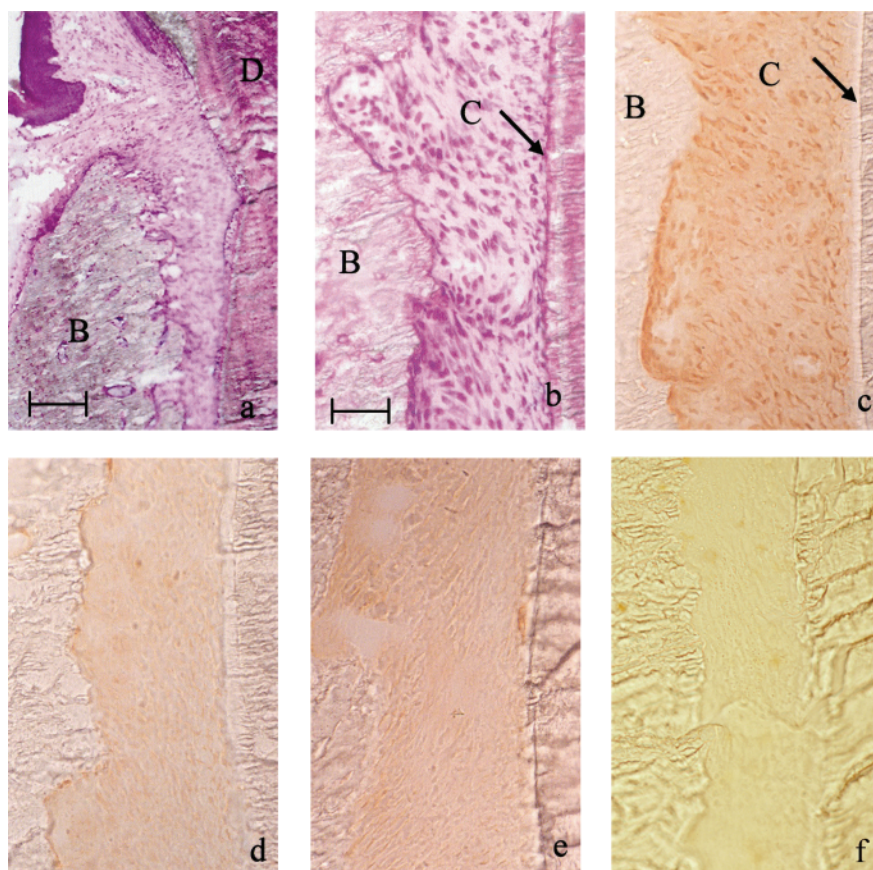
Figure 3 Immunohistochemical localization of transforming growth factor (TGF)-β1, 2, and 3 in the periodontal ligament (PDL). (a and b) Histology of the PDL. Osteoblasts were present on the bone surface and fibroblasts were scattered in the PDL. Cementoblasts were also noted on the cementum surface (arrow). (c, d, and e) Immunohistochemical localization of TGF-β1, 2, and 3. TGF-β1 was localized in the osteoblasts and fibroblasts (c) but less localized in the cementoblasts. TGF-β2 and 3 were not detected in the osteoblasts, fibroblasts, or cementoblasts, (d and e). The negative control of TGF-β1 showed no reactivity (f). (a) ×100 (bar: 20 μm). (b) ×300 (bar: 50 μm). (c, d, e, and f) ×300. B, bone; D, dentine; C, cementum.

Table 1 Result of real-time reverse transcription–polymerase chain reaction; GAPDH, glyceraldehyde 3-posphate dehydrogenase; TGF, transforming growth factor.

RNA expression	
Gene name	Periodontal ligament
GAPDH	6.65 ± 0.33
TGF-β1	36.43 ± 4.97
TGF-β2	Not detected
TGF-β3	Not detected

third of the root, the periodontal fibres were firmly embedded in the cementum and bone and extended regularly, with interlacing among them, from the cementum to the more coronally positioned alveolar bone (Figure 4c and 4d).

Discussion

As adolescent rats, aged 10 weeks, showed an increase in the vertical height of the jaws and also an increase in maxillary and mandibular molar height in the cephalometric analysis of Wistar rats from 15 to 145 days (Hanada, 1967), the formation of roots of the first molar was complete in the present study and the first molars had fully erupted and were in occlusion in the adolescent rat. Therefore, adolescent rats were used to investigate the active eruption (Proffit and Fields, 2000).

TC labelling of the adolescent Wistar rats clearly demonstrated that bone formation occurred on the periosteal and periodontal surfaces of the alveolar bone of the maxillary first molars. A considerable amount of bone apposition occurred at the alveolar crest and apical regions and intraradicular septum (Nakamura *et al.*, 2000). Therefore, the upper first molar had moved downward during the 3 week period, which caused the increase in molar dental height (Hanada, 1967). The results indicate that active
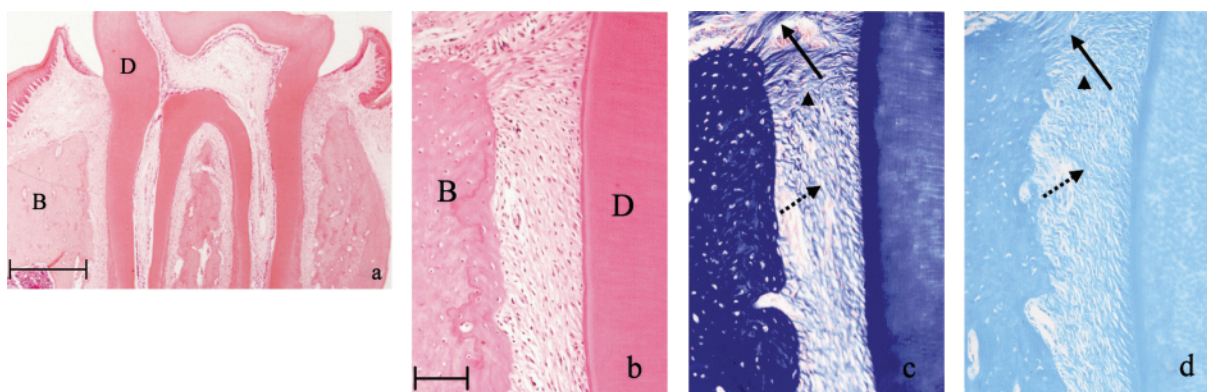
Figure 4 Histology of the periodontal tissues in the decalcified sections. (a and b) Structural relationships of the periodontal tissues were well retained, except for the enamel. (c and d) Three types of periodontal fibres were observed: alveolar crest (arrow), horizontal (arrow head), and oblique (dotted arrow). Each periodontal fibre was well-defined and had a wavy configuration in a functional arrangement. The large arrow indicates the downward direction. (a and b) Haematoxylin and eosin staining, ×20 (bar: 500 µm) and ×100 (bar: 20 µm). (c) Azan stain, ×100. (d) Masson stain, ×100. B, bone; D, dentine.

eruption of the upper first molar (increase in molar dental height) resulted from alveolar bone apposition. It seems that the upper first molar was pushed down by the bone formation at the apical region and intraradicular septum. The bone formation at the crestal regions made it possible to maintain the relationship between the alveolar crest and cemento-enamel junction.

However, despite active eruption (downward movement) of the upper first molars, there was no sign of extension in the periodontal fibre arrangement, which is usually observed in orthodontic tooth movement (Reitan, 1957). All sections from the 10- and 13-week-old rats showed a regular arrangement of periodontal fibres. Azan- and Masson-stained sections demonstrated a regular arrangement of alveolar crest, horizontal, and oblique fibres (Ten Cate, 1996). Therefore, it is reasonable to speculate that new formation of alveolar crest fibres at the alveolar crestal bone and rearrangement of periodontal fibres occur in the PDL. If not, the oblique fibres would run from the bone to the more coronal cementum in accordance with the downward movement of the maxillary first molars, which is one of the characteristic features of orthodontic tooth elongation (Reitan, 1957). The results strongly indicate the importance of the PDL in active eruption and also elucidate why active eruption is not observed around ankylosed teeth (Steiner, 1997; Kofod et al., 2005) and dental implants (Thilander et al., 2001; Rossi and Andreasen, 2003). It seems that orthodontic tooth movement such as depression or elongation of the tooth disarrays bone apposition in alveolar bone, the formation of the alveolar crest fibres and rearrangement of the periodontal fibres, and regulates the vertical height of the tooth, consequently correcting a deep or open bite.

In this study, the real site of rearrangement of the periodontal fibres in the PDL could not be detected. TC labelling lines were observed only in bone and not in cementum except for faint labelling in the apical cementum.

ALP activity was highly detected in the osteoblasts on the bone surface but less on the cementum surface. Furthermore, TGF-β1 was detected in osteoblasts and fibroblasts but less in cementoblasts. It is reasonable to assume that the rearrangement occurs in the PDL on the bone side. This was supported by a report that condensations of ^{3}H-proline-labelled grains were located in the region of the PDL adjacent to the alveolar bone in rats (Oehmke et al., 2004). It also occurs together with formation of alveolar bone. Examination of TGF-β1 in the developing periodontium of the rats demonstrated that TGF-β1 was immunohistochemically located in the fibroblasts and osteoblasts in the cervical PDL and fibroblasts, osteoblasts, and cementoblasts in the apical PDL. This indicates that TGF-β1 may play an important role in the modulation of tissue formation and development of the periodontium (Gao et al., 1998). Furthermore, TGF-β1 increased synthesis of type 1 collagen, fibronectin, and secreted protein, acidic and rich in cystein in a study of PDL cell culture (Fujita et al., 2002). TGF-β1 also supports the proliferation of PDL cells in the study of mitogenic response of cultured cells (Marcopoulou et al., 2003).

The immunoreactivity of TGF-β1 in osteoblasts and fibroblasts in the present study suggests that TGF-β1 plays some role in the formation of alveolar crest fibres and rearrangement of the PDL even after formation of the PDL.

RT-PCR clearly demonstrated that the cells in periodontal tissues contain only mRNA of TGF-β1. Microdissected PDL is likely to contain cells other than fibroblasts. However, the number of fibroblasts was much greater than that of other cells, which means that mRNA of the PDL is mainly derived from fibroblasts. The results indicate that TGF-β1, immunohistochemically detected in the fibroblasts, was synthesized within the fibroblasts and not endocytosed from the extracellular matrix. In addition, TGF-β1 is synthesized in the fibroblast not only during the development

of the PDL but also during the normal functional state of the PDL in adolescent rats.

However, no specific role for TGF-β1 was observed in the formation of alveolar crest fibres and rearrangement of the periodontal fibres. Recent reports suggest that periostin, a secreted protein that is expressed in the early stage of osteoblastic cells (Afanador *et al.*, 2005), and growth differentiation factors (Sena *et al.*, 2003) belonging to the TGF-β super family might be involved in the development and arrangement of the periodontal fibres. Periostin expression appears to be up-regulated by TGF-β1 (Horiuchi *et al.*, 1999). Therefore, TGF-β1 would be closely involved in the mechanism of this active eruption.

In this study, TGF-β2 and 3 were not detected by immunohistochemistry or with RT-PCR. TGF-β2 and 3 are implicated in pathological conditions, such as inflammation, tissue scarring, and fibrosis in wound healing (Polo *et al.*, 1997; Brahmatewari *et al.*, 2000; Bayat *et al.*, 2005). The vertical alveolar bone growth and rearrangement of the PDL are physiological processes, in which TGF-β2 and 3 may not be involved.

Conclusion

The results of the present study suggest that active eruption occurs mainly by alveolar bone formation concomitant with formation of alveolar crest fibres and rearrangement of periodontal fibres in the PDL.

Funding

References

Afanador E *et al.* 2005 Messenger RNA expression of periostin and Twist transiently decrease by occlusal hypofunction in mouse periodontal ligament. Archives of Oral Biology 50: 1023–1031

Arai C, Ohnuki Y, Umeki D, Saeki Y 2005 Effect of bite opening and cyclosporine A on the mRNA level of myosin heavy chain and the muscle mass in rat masseter. Journal of Physiological Sciences 55: 173–179

Bayat A, Walter J M, Bock O, Mrowietz U, Ollier W E, Ferguson M W 2005 Genetic susceptibility to keloid disease: mutation screening of the TGFbeta3 gene. British Journal of Plastic Surgery 58: 914–921

Brahmatewari J, Serafini A, Serralta V, Mertz P M, Eaglstein W H 2000 The effect of topical transforming growth factor-beta2 and anti-transforming growth factor-beta2, 3 on scarring in pigs. Journal of Cutaneous Medicine and Surgery 4: 126–131

Enlow D H (ed.) 1990 The facial growth process. In: Facial growth, 3rd edn. W.B. Saunders Co, Philadelphia, pp. 118–121.

Fujita T, Shiba H, Sakata M, Uchida Y, Ogawa T, Kurihara H 2002 Effects of transforming growth factor-β1 and fibronectin on SPARC expression in cultures of human periodontal ligament cells. Cell Biology International 26: 1065–1072

Gao J, Symons A L, Bartold P M 1998 Expression of transforming growth factor beta 1 (TGF-β1) in the developing periodontium of rats. Journal of Dental Research 77: 1708–1716

Graber T M (ed.) 1972 Growth and development. In: Orthodontics, principles and practice. W.B. Saunders Co, Philadelphia, pp. 75–86.

Hanada K 1967 A study on growth and development of the dentofacial complex of the living rat by means of longitudinal roentgenographic cephalometrics. The Journal of the Stomatological Society, Japan 34: 18–74

Horiuchi K, Amizuka N, Takeshita S, Takamatsu H, Katsuura M, Kudo A 1999 Identification and characterization of a novel protein, periostin, with restricted expression to periosteum and periodontal ligament and increased expression by transforming growth factor ß. Journal of Bone and Mineral Research 14: 1239–1249

Kawamoto T 2003 Use of a new adhesive film for the preparation of multi-purpose fresh frozen sections from hard tissues, whole-animals, insects and plants. Archives of Histology and Cytology 66: 123–143

Kofod T, Würtz V, Melsen B 2005 Treatment of an ankylosed central incisor by single tooth dento-osseus osteotomy and a simple distraction device. American Journal of Orthodontics and Dentfacial Orthopedics 127: 72–80

Marcopoulou C E, Vavouraki H N, Dereka X E, Vrotsos I 2003 Proliferative effect of growth factors TGF-beta1, PDGF-BB and rhBMP-2 on human gingival fibroblasts and periodontal ligament cells. Journal of the International Academy of Periodontology 5: 63–70

Mayahara H, Hirano H, Saito T, Ogawa K 1969 The new lead citrate method for the ultracytochemical demonstration of activity on non-specific alkaline phosphatase. Histochemistry and Cell Biology 11: 88–96

Nakamura Y, Tanaka T, Wakimoto Y, Noda K, Kuwahara Y 1994 Preparation of unfixed and undecalcified frozen section of adult rat periodontal ligament during experimental tooth movement. Biotechnic and Histochemistry 69: 186–191

Nakamura Y *et al.* 2000 Histology and tetracycline labeling of a single section of alveolar bone of first molars in the rat. Biotechnic and Histochemistry 75: 1–6

Nakamura Y *et al.* 2007 Laser capture microdissection of rat periodontal ligament for gene analysis. Biotechnic and Histochemistry 82: 295–300

Oehmke M J, Schramm C R, Knolle E, Frickey N, Bernhart T, Oehmke H J 2004 Age-dependent changes of the periodontal ligament in rats. Microscopy Research and Technique 63: 198–202

Polo M, Ko F, Busillo F, Cruse C W, Krizek T J, Robson M C 1997 Cytokine production in patients with hypertrophic burn scars. The Journal of Burn Care & Rehabilitation 18: 477–482

Proffit W R, Fields Jr H W 2000 The development of orthodontic problems. In: Proffit W R (ed). Contemporary orthodontics, 3rd edn. Mosby, St Louis, pp. 106–108.

Reitan K 1957 Some factors determining the evaluation of force in orthodontics. American Journal of Orthodontics 43: 32–45

Rossi E, Andreasen J Q 2003 Maxillary bone growth and implant positioning in a young patient. The International Journal of Periodontics & Restorative Dentistry 23: 113–119

Sena K, Morotome Y, Baba O, Terashima T, Takano Y, Ishikawa I 2003 Gene expression of growth differentiation factors in the developing periodontium of rat molars. Journal of Dental Research 82: 166–171

Shaddy R E, Zhangb Y L, White W L 1996 Murine and pediatric myocardial growth factor mRNA expression using reverse transcription-polymerase chain reaction. Biochemical and Molecular Medicine 57: 10–13

Schudy F F 1965 The rotation of the mandible resulting from growth: its implications in orthodontic treatment. Angle Orthodontist 35: 36–50

Steiner D R 1997 Timing of extraction of ankylosed teeth to maximize ridge development. Journal of Endodontics 23: 242–245

Ten Cate A R 1996 Periodontium. In: Ten Cate A R, Freeman E (eds). Oral histology, 4th edn. Mosby, St Louis, pp. 335–372.

Thilander B, Ödman J, Lekholm U 2001 Orthodontic aspects of the use of oral implants in adolescents: a 10-year follow-up study. European Journal of Orthodontics 23: 715–731

Zhao J, Araki N, Nishimoto S K 1995 Quantitation of matrix Gla protein mRNA by competitive polymerase chain reaction using glyceraldehydes-3-phosphate dehydrogenase as an internal standard. Gene 155: 159–165